Structure, Volume *26*

Supplemental Information

A Hyperthermophilic Phage Decoration Protein Suggests Common Evolutionary Origin with Herpesvirus Triplex Proteins and an Anti-CRISPR Protein

Nicholas P. Stone, Brendan J. Hilbert, Daniel Hidalgo, Kevin T. Halloran, Jooyoung Lee, Erik J. Sontheimer, and Brian A. Kelch

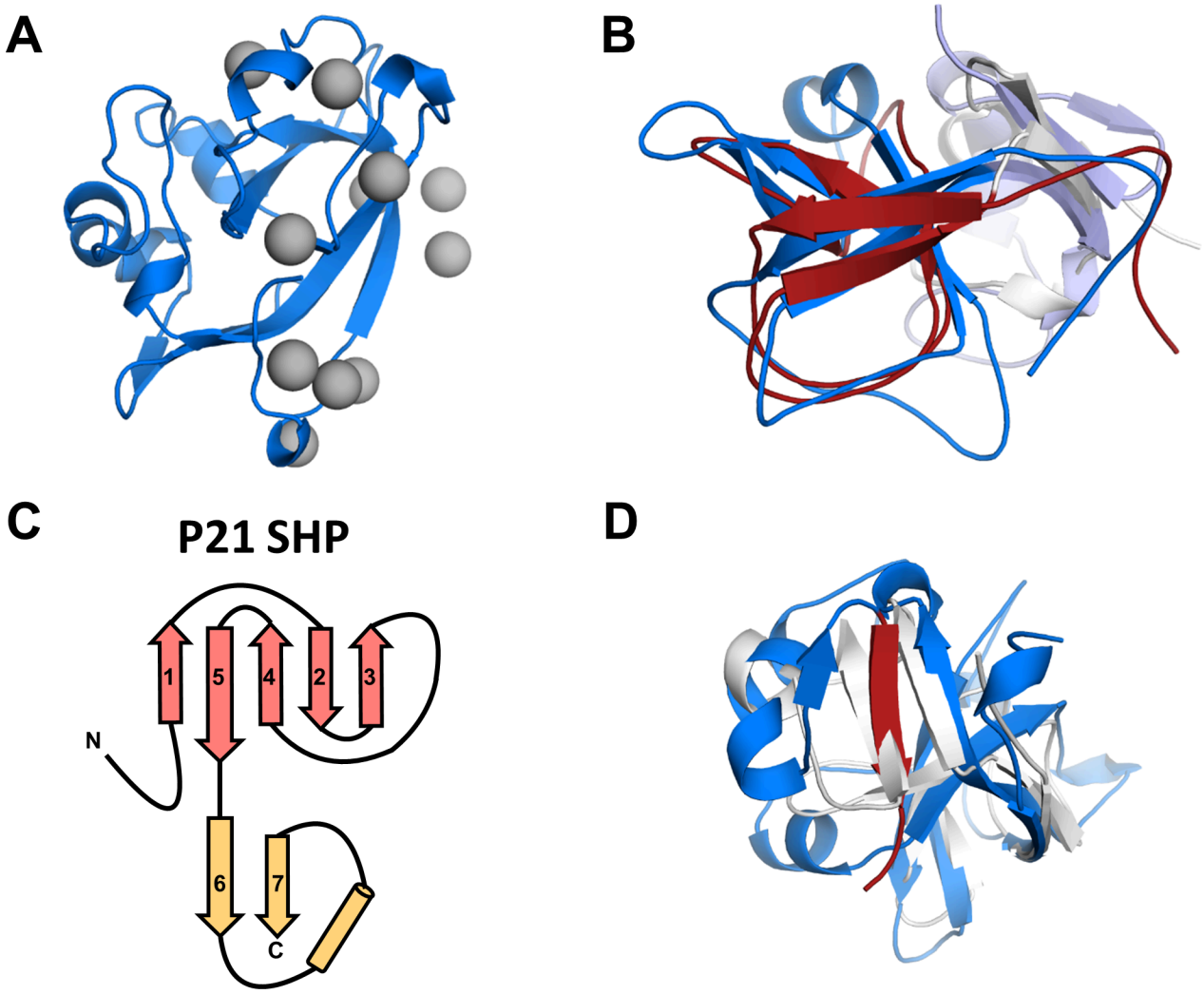

E

```
P74-26    17 RVPRLHAYG-VFALPFPMDPDVEWGNWFAGPHPKAFLVSVHPSGPKAGHVYPTDLSDPDSVANVIGMV
P23-45    17 RVPRLHAYG-VFALPFPMDPDVNWAQWFTGPHPRAFLVSIHKYGPKAGHVYPTNLTDEDALLNVIGMV
G20c      17 RVPRLHAYG-VFALPFPMDPDVEWGNWFAGPHPKAFLVSVHPSGPKAGHVYPTDLSDPDSVANVIGMV
Lambda    15 ------SDPAH-TATAPGGLS--AK-AP-----AMTPLMLD-TSS--RKLVAWDGTT---DGAAVGIL
P21       18 ------NDPAH-TATGSSGIS--SP-TP-----ALTPLMLD-EAT--GKLVVWDGQK---AGSAVGIL
N15       15 ------SDPAH-TAYGPGELT--AS-TP-----AMTPLMLD-ATS--GKLTVWDGAH---AGAATGIL
HK225     15 ------SDPAH-TAYGLGELT--AS-TP-----AMTPLMLD-ATS--GKLAVWDGAH---AGAAMGIL

P74-26    84 LDGHDYEADHNVTVTLRAAVPI-EYVQQGIEAPPLQPDPAVLNAAPQLK----LKVIKGHYFFDYTR
P23-45    84 LDGHDYENDPNVTVTLKAAVPI-EYVQQDPQAPALQPHQAVLDAAEVLK----LKVIKGHYFFDYTR
G20c      84 LDGHDYEADHNVTVTLRAAVPI-EYVQQGVELPPLQPDPAVLNAAPQLK----LKVIKGHYFFDYTR
Lambda    62 AVAADQT-STTLTFYKSGTF-RYEDVLWPEAASD------ETKKRTAFAGTAISIV----------
P21       65 VLPLEGT-ETALTYYKSGTF-ATEAIHWPESV-D------EHKKANAFAGSALSHAALP--------
N15       62 AVTADQN-SAELAFYKSGSF-RIEDVLWPSAVTD------ENIKRNAFAGTAISIV----------
HK225     62 AVTADQN-SAELAFYKSGSF-RIEDVLWPSAVTD------DNIKRNAFAGTAISIV----------
```

Supplementary Figure 1. Structural characterization of P74-26 gp87 reveals conserved β-tulip domain, Related to Figures 1 and 2.

A) Iodide ion binding positions are shown mapped onto 1.7-Å structure of P74-26 gp87 (iodides in grey).

B) Structural alignment of gp87 (β-tulip in blue) with the decoration protein SHP from phage P21 (white, β-tulip in red, PDB: 1TD3).

C) Topology diagram of the P21 decoration protein SHP.

D) Structural alignment of P74-26 gp87 (blue) with λ gpD (grey) highlighting additional strand in gp87 (red) forming an antiparallel β-sheet in the C-terminal domain.

E) Structure-based multiple sequence alignment of thermophilic and mesophilic decoration proteins reveals conserved residues. Thermophilic and mesophilic decoration proteins are color coded red and blue, respectively.

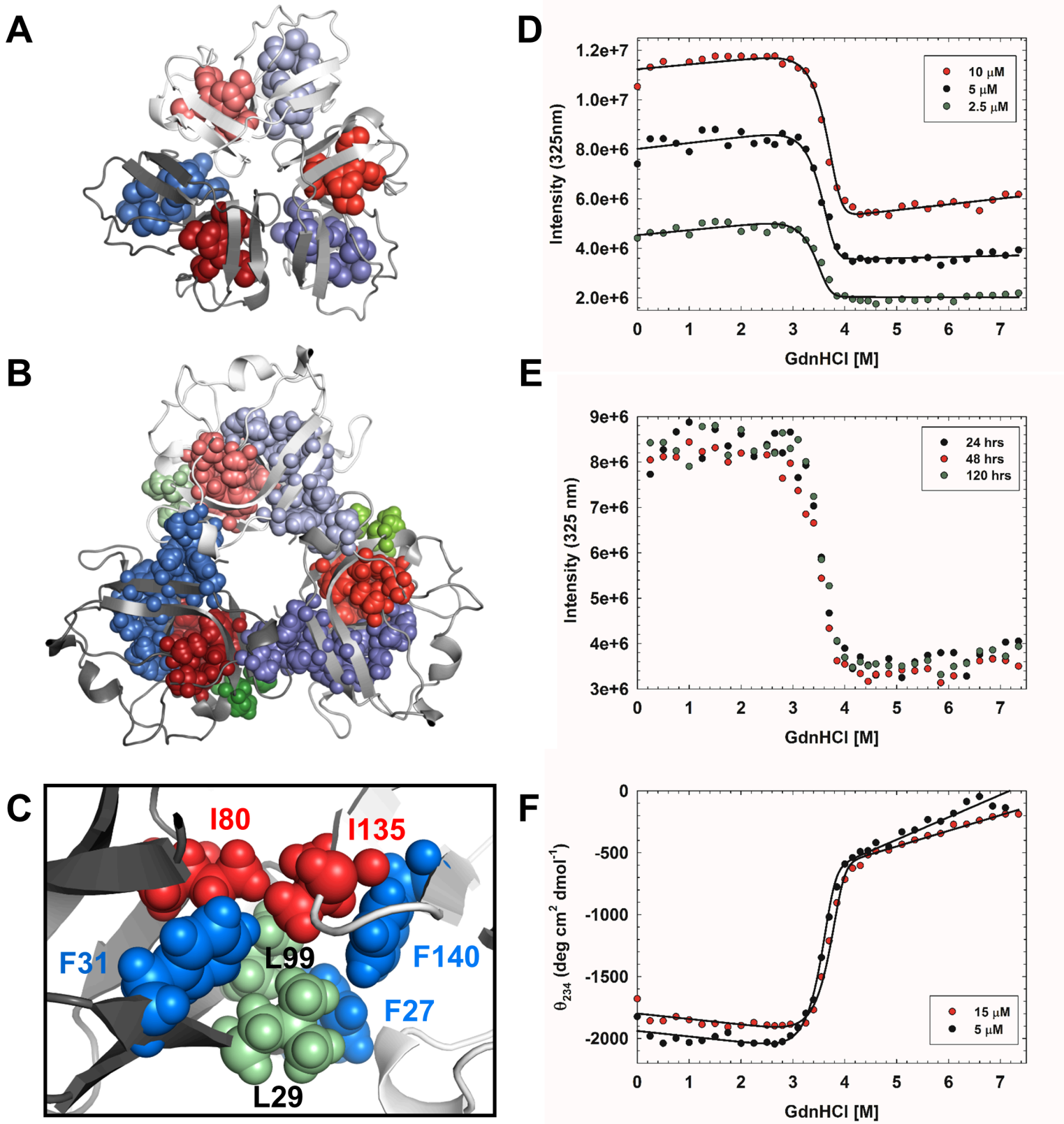

Supplementary Figure 2. P74-26 gp87 forms a stable trimer using extensive hydrophobic networks, Related to Figure 3.

A) Hydrophobic ILVF clusters mapped onto the structure of λ gpD trimer show clusters within the β-tulip (blue) and C-terminal domains (red) that are unconnected to each other.

B) ILVF clusters mapped onto the P74-26 gp87 trimer show an extended hydrophobic network, with clusters forming intermolecular and intramolecular interactions (clusters shown in blue span multiple subunits).

C) gp87 β-tulip domains interact with neighboring subunits primarily through hydrophobic interactions, forming an intermolecular cluster consisting of Ile (red), Leu (green), and Phe (blue) residues.

D) Equilibrium unfolding of gp87 at monomer concentrations of 10 μM (red), 5 μM (black), and 2.5 μM (cyan) was monitored by tryptophan fluorescence; excitation 295 nm, emission 325 nm.

E) Equilibrium unfolding of gp87 after incubation for 24 hours (black), 48 hours (red), and 120 hours (cyan) (independent experiments) shows equilibrium is reached after 24 hours.

F) Equilibrium unfolding of gp87 at monomer concentrations of 5 μM (black) and 15 μM (red) monitored by circular dichroism at 234 nm. Solid lines represent the fit to a model of trimer to three unfolded monomers in A, C.

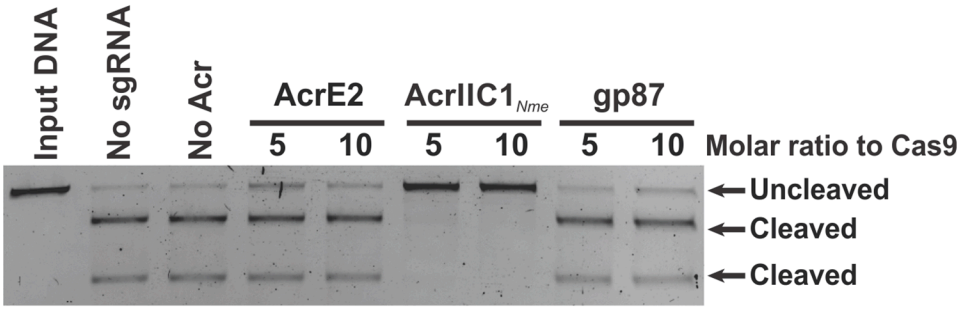

Supplementary Figure 3. gp87 does not inhibit DNA cleavage by NmeCas9 *in vitro, Related to Figure 5*.
Linearized plasmid DNA bearing a protospacer (target) next to a PAM sequence was subjected to *in vitro* cleavage by purified NmeCas9. NmeCas9 was pre-incubated with purified anti-CRISPR proteins AcrIIC1$_{Nme}$ and AcrE2 as a positive and negative control, respectively. Molar ratios of anti-CRISPR protein or gp87 relative to NmeCas9 are shown at the top of each lane. Input DNA and cleaved products are indicated with arrows on the right. The NmeCas9 cleavage assays shown are representative of three independent replicates.

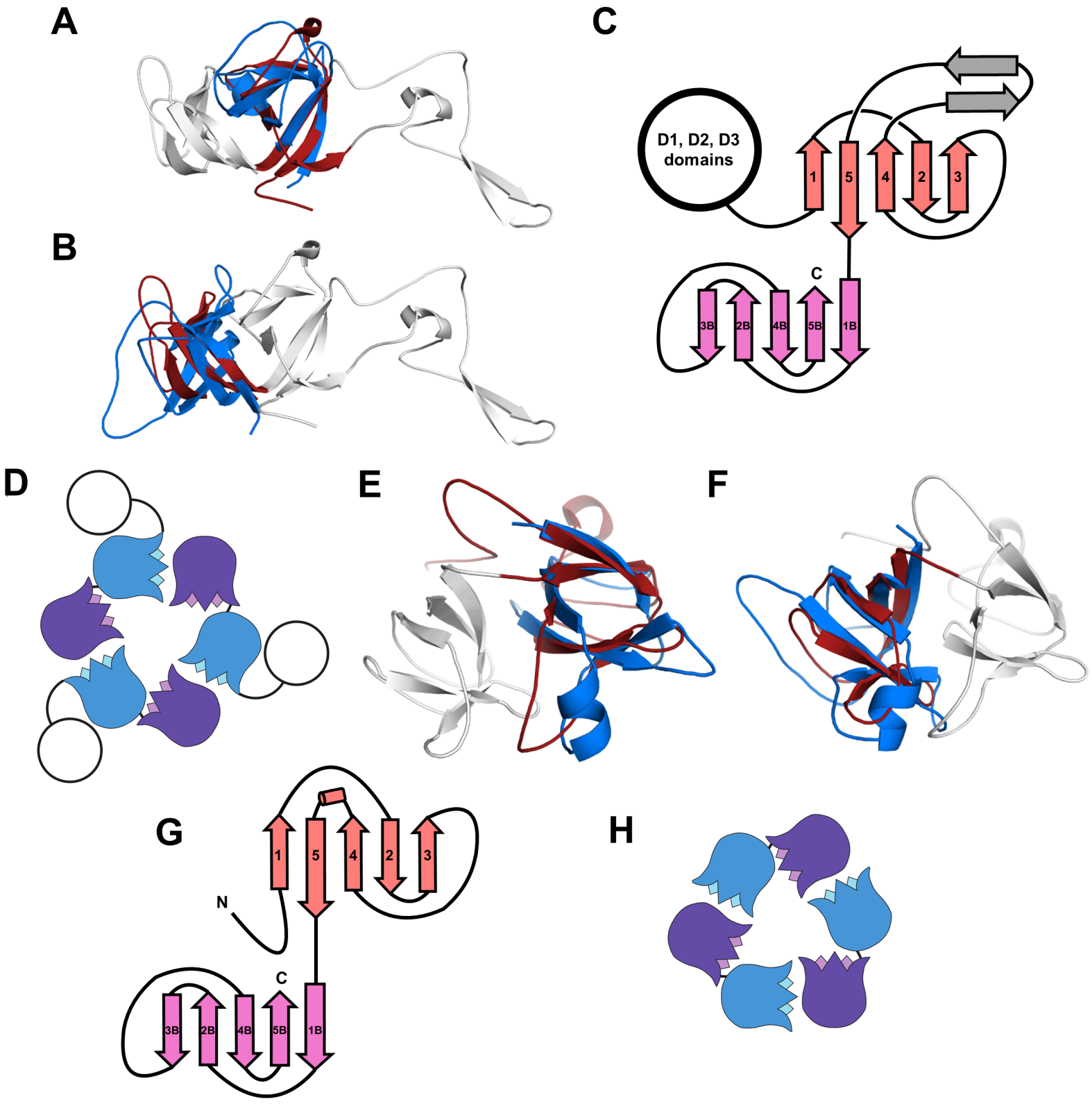

Supplementary Figure 4. Conservation of the β-tulip domain in the decoration protein from marine siphovirus TW1 and Φ29 tailspike protein, Related to Figures 1 and 4.

A) Structure-based alignment of P74-26 gp87 β-tulip domain (blue) with the N-terminal β-tulip domain (red) of the D4 domain of Φ29 tailspike protein gp12.

B) Alignment of P74-26 gp87 β-tulip domain with the C-terminal β-tulip domain of gp12.

C) Topology diagram of Φ29 gp12 shows the orientation of the tandem β-tulip domains.

D) Model of the head-to-tail β-tulip domain orientation in gp12.

E) Structure-based alignment of gp87 β-tulip domain (blue) with the N-terminal β-tulip domain from TW1 gp56 (red).

F) Structure-based alignment of gp87 β-tulip domain (blue) with the C-terminal β-tulip domain from TW1 gp56 (red).

G) Topology diagram of TW1 gp56 shows the orientation of the tandem β-tulip domains.

H) Model of the β-tulip domain orientation in TW1 gp56.

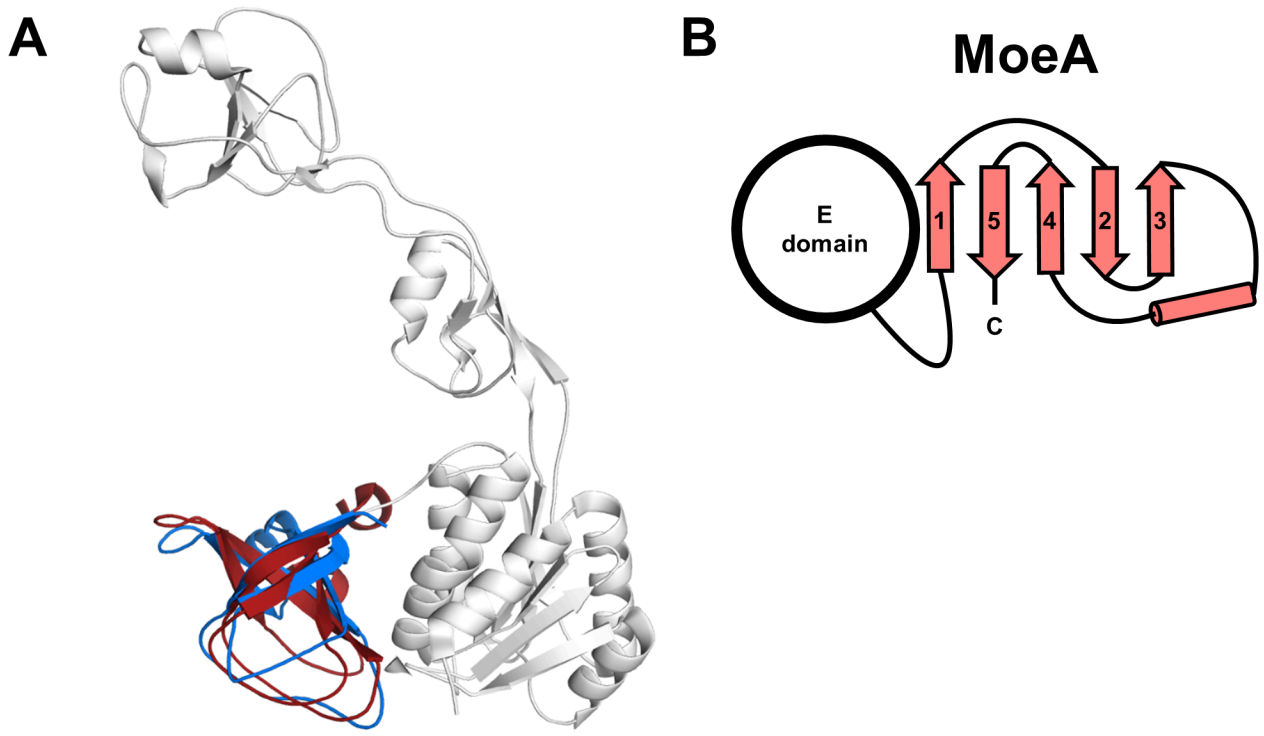

Supplementary Figure 5. Conservation of β-tulip domain in the Moco biosynthesis enzyme MoeA, Related to Figures 1 and 4.

A) Structure-based alignment of P74-26 β-tulip domain (blue) with Moe1 (grey, β-tulip in red, PDB: 2NQQ).

B) Topology diagram of MoeA E-region.

	P74-26 gp87	Lambda gpD	P21 SHP	HCMV Tri1	HCMV Tri2	Anticrispr AcrIIC1	φ29 gp12 (N-term)	φ29 gp12 (C-term)	TW1 gp56 (N-term)	TW1 gp56 (C-term)
Lambda gpD	N_{aln}: 54 RMSD: 2.12 Z score: 8.4									
P21 SHP	N_{aln}: 55 RMSD: 1.96 Z score: 8.0	N_{aln}: 54 RMSD: 0.79 Z score: 9.7								
HCMV Tri1	N_{aln}: 53 RMSD: 2.40 Z score: 3.4	N_{aln}: 48 RMSD: 2.43 Z score: 4.2	N_{aln}: 46 RMSD: 2.38 Z score: 4.0							
HCMV Tri2	N_{aln}: 43 RMSD: 2.24 Z score: 4.9	N_{aln}: 44 RMSD: 2.24 Z score: 6.0	N_{aln}: 44 RMSD: 2.36 Z score: 6.2	N_{aln}: 43 RMSD: 1.64 Z score: 4.9						
Anticrispr AcrIIC1	N_{aln}: 45 RMSD: 2.61 Z score: 3.8	N_{aln}: 38 RMSD: 3.07 Z score: 3.8	N_{aln}: 37 RMSD: 2.94 Z score: 3.2	N_{aln}: 38 RMSD: 2.29 Z score: 2.7	N_{aln}: 39 RMSD: 2.63 Z score: 3.6					
φ29 gp12 (N-term)	N_{aln}: 39 RMSD: 1.70 Z score: 5.1	N_{aln}: 46 RMSD: 2.03 Z score: 5.3	N_{aln}: 47 RMSD: 1.92 Z score: 6.4	N_{aln}: 46 RMSD: 2.65 Z score: 3.7	N_{aln}: 46 RMSD: 2.16 Z score: 4.0	N_{aln}: 43 RMSD: 3.03 Z score: 2.5				
φ29 gp12 (C-term)	N_{aln}: 45 RMSD: 1.51 Z score: 6.6	N_{aln}: 42 RMSD: 2.08 Z score: 5.4	N_{aln}: 42 RMSD: 2.04 Z score: 5.0	N_{aln}: 45 RMSD: 2.38 Z score: 5.1	N_{aln}: 42 RMSD: 2.16 Z score: 5.6	N_{aln}: 40 RMSD: 2.27 Z score: 3.5	N_{aln}: 44 RMSD: 2.97 Z score: 2.9			
TW1 gp56 (N-term)	N_{aln}: 54 RMSD: 2.77 Z score: 4.5	N_{aln}: 49 RMSD: 2.27 Z score: 4.8	N_{aln}: 51 RMSD: 2.22 Z score: 4.2	N_{aln}: 46 RMSD: 2.81 Z score: 2.1	N_{aln}: 43 RMSD: 2.59 Z score: 3.9	N_{aln}: 40 RMSD: 2.98 Z score: 3.0	N_{aln}: 46 RMSD: 1.78 Z score: 5.7	N_{aln}: 48 RMSD: 2.76 Z score: 2.5		
TW1 gp56 (C-term)	N_{aln}: 53 RMSD: 2.29 Z score: 4.8	N_{aln}: 51 RMSD: 1.57 Z score: 6.7	N_{aln}: 52 RMSD: 1.47 Z score: 7.7	N_{aln}: 48 RMSD: 2.26 Z score: 4.0	N_{aln}: 42 RMSD: 1.84 Z score: 5.7	N_{aln}: 39 RMSD: 2.92 Z score: 2.9	N_{aln}: 50 RMSD: 1.92 Z score: 6.3	N_{aln}: 48 RMSD: 2.09 Z score: 6.7	N_{aln}: 52 RMSD: 2.46 Z score: 4.2	
MoeA	N_{aln}: 54 RMSD: 2.44 Z score: 4.7	N_{aln}: 48 RMSD: 2.53 Z score: 4.2	N_{aln}: 50 RMSD: 2.94 Z score: 4.3	N_{aln}: 47 RMSD: 3.13 Z score: 2.6	N_{aln}: 39 RMSD: 2.54 Z score: 4.6	N_{aln}: 44 RMSD: 2.67 Z score: 4.9	N_{aln}: 44 RMSD: 2.78 Z score: 4.6	N_{aln}: 45 RMSD: 2.45 Z score: 4.1	N_{aln}: 55 RMSD: 3.38 Z score: 2.2	N_{aln}: 54 RMSD: 2.50 Z score: 4.2

Table S1, Related to Figures 1, 4, and 5. C_α RMSD comparison of β-tulip domains. RMSD values are reported in Å; N_{aln} = number of residues aligned for each comparison.